

Analysis of the maximum extractable power of photonic crystal fiber lasers

Kai Guo (郭凯), Xiaolin Wang (王小林), Cheng Luo (罗成), Pu Zhou (周朴),
and Bohong Shu (舒柏宏)*

College of Optoelectronics Science and Engineering, National University of Defense Technology,
Changsha 410073, China

*Corresponding author: shu_bh@tom.com

Received March 25, 2014; accepted May 3, 2014; posted online October 20, 2014

In this article, we analyze the factors that limit the output power increase for photonic crystal fiber lasers and set a theoretical model to calculate the maximum extractable power of ytterbium-doped photonic crystal fibers. Numerically, when the diameter of core is 76- μm and the pumping intensity is 0.21 W/($\mu\text{m}^2 \times \text{Sr}$), the output of pure silica and ytterbium-doped photonic crystal fiber lasers is 100-kW, considering the technology for the time being. The main limitations of power scaling are facet damage and thermal self-focusing. In case of the strict single-mode operation condition, the maximum extractable power is 100-kW when the numerical aperture is 0.05. Considering the strict single-frequency operation condition, the maximum extractable power of both pure silica and ytterbium-doped photonic crystal fiber lasers is 1.65-kW, where the main factor is stimulated Brillouin scattering effect. Compared with the previous results, the increase in the maximum extractable power depends on three parameters: the availability of high-brightness pump diodes, the endless single-mode characteristic of the photonic crystal fiber, and the high doping density which lead to efficient absorption coefficient of pumping light. Finally, we simulate numerical aperture that influences the maximum power of photonic crystal fiber lasers and compare the difference in maximum output power of photonic crystal fibers and double-cladding fiber lasers in single-frequency condition.

OCIS codes: 140.3280, 140.4480, 140.3510, 140.3500.

DOI: 10.3788/COL201412.S21411.

Fiber lasers and amplifiers with excellent beam quality and high efficiency have been widely developed in recent years^[1]. Photonic crystal fiber (PCF) is a special class of fiber with designable structure and controllable characteristics. Since Russell and coworkers^[2] at Max-Planck-Institute made the first PCF in 1996, applications about PCF came into being from many aspects^[3-8]. In pure silica fibers, the refractive index can be controlled by varying the air hole diameter, PCF can have a heavy density of rare-earth-doped PCF despite the influences of germanium (Ge) and boron (B). Compared with double-cladding fibers (DCF), PCFs have high Raman threshold and high Brillouin threshold, which help reduce the limitations of nonlinear effects. The designable structure enables PCFs to have the endless single-mode property^[4]. Highly doped PCFs can be used in all-fiber lasers applications and a high level of the maximum extractable power can be obtained with a short PCF. Besides, the attractive controllable nonlinear properties and larger single-mode cores open up a range of opportunities for further application. Recent results indicate that PCFs offer vast potential to enhance the performance of next-generation laser systems^[5]. Therefore, it is necessary to analyze the characteristics of the doped PCFs in high-power applications systematically.

As theoretical models set up in 2008^[9], the maximum extractable power of fiber lasers can be determined on the basis of six parameters: thermal effect including thermal fracture, core melting, thermal lens effect, optical effect, nonlinear optical effect, and pumping brightness. The distribution of heat will change the refractive

index of fiber cross-section that the transverse of laser will focus as if a lens has been employed. When heat continues to accumulate and levels off at a high density, it may damage the surface structure and melt the core, thereby causing the core melting and the thermal fracture^[10,11]. The optical effect damages the fiber endface by laser beams directly. In wide spectrum lasers and amplifiers, stimulated Raman scattering (SRS) effect is considered, whereas stimulated Brillouin scattering (SBS) effect is more dominant in single-frequency lasers. The brightness of pump source will limit the pumping light coupling into fiber and determine the output power directly. These factors can be described by the following formulas, where a , b , and L are the radius of core, the radius of inner cladding, and the length of PCF, respectively^[9]:

$$\frac{\eta_{\text{laser}} \pi R_m L}{\eta_{\text{heat}} \left[1 + \left(2k/bh \right) + 2 \ln(b/a) \right]} \quad (1)$$

$$P_2 = \frac{4\eta_{\text{laser}} \pi k (T_m - T_c) L}{\eta_{\text{heat}} \left[1 + \left(2k/bh \right) + 2 \ln(b/a) \right]}, \quad (2)$$

$$P_3 = \frac{\eta_{\text{laser}} \pi \kappa \lambda^2 L}{2\eta_{\text{heat}} (dn/dT) a^2}, \quad (3)$$

$$P_4 \approx \frac{16\pi a^2 Q^2 \ln(G)}{g_R L}, \quad (4)$$

$$P_5 = Q^2 a^2 \pi I_{\text{damage}}, \quad (5)$$

$$P_6 = \eta_{\text{laser}} I_{\text{pump}} \pi^2 (\text{NA})^2 \frac{\alpha_{\text{core}}}{A} L a^2, \quad (6)$$

$$P_7 = \frac{17\pi a^2 Q^2 \ln(G)}{g_B L}. \quad (7)$$

The simulation of output power has the following steps:

- 1) Vary the radius and fiber length and record the maximum extractable power influenced by six factors, respectively.
- 2) Compare the output power and choose the minimum one influenced by each factor.
- 3) Record the main reason of output power limitation.
- 4) Consider the single-frequency laser and repeat Steps (1)–(4).

All the parameters are listed in Table 1. The thermal parameters are mainly obtained from the study by Dawson *et al.*^[9], whereas other parameters, except pumping brightness, are obtained from the data in commercial fiber products. As a result of calculation

of two commercial pumping sources, the brightness of recent levels off at $0.2 \text{ W}/(\mu\text{m}^2 \times \text{Sr})$ ^[12] and more than $2 \text{ W}/(\mu\text{m}^2 \times \text{Sr})$ ^[13] in wide spectrum condition, which means that brightness has improved at least 10 times in the past 5 years. Considering the acceptable results of simulation, we calculate the maximum extractable power of our model choosing the pumping brightness of $0.21 \text{ W}/(\mu\text{m}^2 \times \text{Sr})$. As outlined in commercial products, the absorption coefficient of PCF can reach 650 dB/m ^[14] with a flexible structure. Although in actual application it is not possible to use PCF with such a high absorption coefficient, our simulation is just a way to provide analysis in ideal way.

Using the parameters given in Table 1, we complete the simulation of the maximum extractable power with the core diameter varying from 0 to $80\text{-}\mu\text{m}$ and the fiber length varying from 0 to 80 m . The limitation of PCF laser output power is 97.09-kW , nearly three times to that of DCF laser (36.6-kW). Compared with the results of Dawson *et al.*^[9], the increase of the maximum extractable power is due to the increase in laser diode brightness, which is 10 times than it used to be 5 years ago, and the high doping density, which can be seen from the great breakthrough of the absorption coefficient of the fiber core.

As shown in Fig. 1(a), when the core diameter of PCF is less than $20\text{-}\mu\text{m}$, the output power depends mainly on the pumping brightness. If the diameter

Table 1. Parameters and Values used in Simulation

Parameter	Symbol	Value	Unit
Rupture Modulus of Silica Glass	R_m	2460	W/m
Thermal Conductivity	k	1.38	W/(m K)
Convective Film Coefficient for Cooling Fiber	h	10^{-4}	W/(m ² K)
Melt Temperature of Fused Silica	T_m	1983	K
Change in Index with Temperature	$\frac{dn}{dT}$	11.8×10^{-6}	1/K
Peak Raman Gain Coefficient in Pure Silica PCF	g_R	10^{-13}	m/W
Peak Brillouin Gain Coefficient in Pure Silica PCF	g_B	5×10^{-11}	m/W
Small Signal Pump Absorption of Laser r	A	20	dB
Assumed Laser Gain	G	10	—
Ratio of the Mode Field Radius to the Core Radius	Q	0.8	—
Optical Damage Limit	I_{damage}	10	W/ μm^2
Environmental Temperature	T_c	300	K
Pump Brightness Limit	I_{pump}	0.21	W/ $(\mu\text{m}^2 \times \text{Sr})$
Peak Core Absorption at Pump Wavelength	α_{core}	650	dB/m
Fraction of Pump Light Converted to Laser Power	η_{laser}	0.85	—
Fraction of Pump Light Converted to Heat	η_{heat}	0.1	—
Laser Wavelength	λ	1064	nm
Numerical Aperture of Inner Cladding	NA	0.46	—

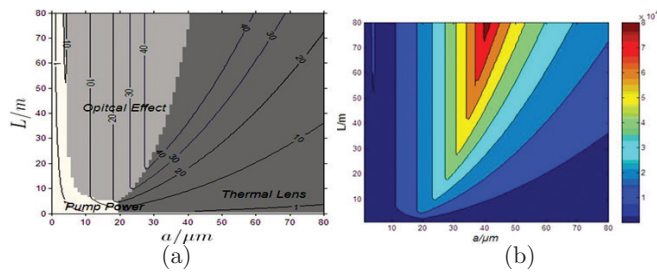


Fig. 1. (a) Output power and physical limits allowing the core diameter and fiber length to vary. (b) Output power of wide spectrum core diameter and PCF length varying.

increases, the thermal lens effect will limit mostly. It is also shown that with the increasing length, the optical effect on the maximum extractable power also increases.

Figure 1(b) is the output power distribution with varying core diameter and PCF lens. It is obvious that simply increasing the core diameter will not increase the output power. We can get a laser output by using an 80-m PCF with core diameter of 76 μm . In addition, the maximum extractable power we could maintain is a single-mode output for the sake of the endless single-mode characteristic of PCF. It is attractive as the maximum power of DCF in Ref. [9] was working in multi-mode condition.

As shown in Fig. 2(a), the output power of lasers or amplifiers working in single-frequency condition is mainly affected by the SBS effect. The thermal lens effect is observed only when the core diameter is greater than 30- μm . The output power of strict single-frequency laser is 1.65-kW. Compared with the result of Dawson *et al.*^[9], the maximum output power is less in our simulation, which is because Dawson used a spectrum width single-frequency condition whereas in our model it is stricter.

Figure 2(b) describes the output power distribution in single-frequency condition. The maximum extractable power will be highest when the core diameter reaches 40- μm . This is because the SBS effect will decrease with the increasing core diameter, thereby lowering the energy density. Although the maximum output power is limited, we can obtain large power throughout several experimental methods by decreasing the SBS effect, which is simply ignored in our simulation^[15].

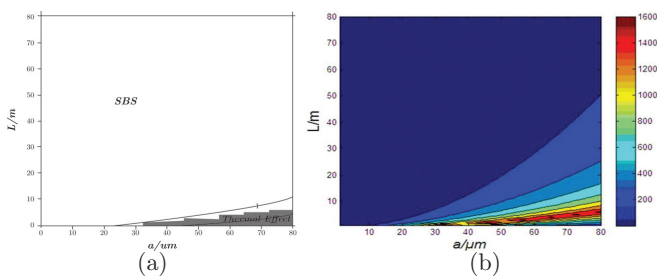


Fig. 2. (a) Single-frequency output power and physical limits allowing the core diameter and fiber length to vary. (b) Single-frequency output power with core diameter and PCF length varying.

The numerical aperture (NA) of inner cladding will affect the ability of the PCF to confine light. Researches about the relationship between the maximum extractable power and the core NA tend to focus mainly on the single-mode condition. In the PCF, the relative refractive index is controlled by designing the size and the position of the air hole, which make it possible to get an endless single-mode laser, not limiting the output power. However, the inner-cladding NA affects the absorption coefficient of the pump light. Designing the structure should we consider the inner cladding NA and it is necessary to compare the difference when the inner cladding NA varying.

Figure 3 shows four lines about the output power with core diameter 18- μm and the PCF length varying. Choosing this fitful diameter will lead to a good sight of comparison with inner-cladding NA 0.4, 0.5, 0.6, and 0.7. Figure 3 shows that the output power increases with increasing PCF length. The maximum extractable power increases rapidly with increasing inner-cladding NA. Considering the parameters we choose, the maximum extractable power now can be more than 10-kw. The maximum value independent thus the increasing rate will vary with the cladding. Thus, it is clear that we can get high power output by using large inner-cladding NA rather than by increasing length.

Figure 4 shows that PCF and DCF, which share the same parameters, have quite different characteristics in single-frequency condition. As shown in the figure, the maximum single-frequency laser output is the same. The result is different from the results of Dawson *et al.*^[9] as we have used a more strict single-frequency condition. Although the maximum output powers are the same, they have different characteristics with the varying fiber lengths. In PCF lasers, the maximum extractable power increases with the increasing length, and then decreases when the fiber length reaches approximately 4.6 m. However, the DCF output power decreases monotonously when the fiber length overtakes approximately 0.3 m. In PCF lasers, the diameter can be large irrespective of the multimode condition, so the SBS threshold is higher than that in the DCF lasers of the same length. Besides, pure silica PCFs may have lower SBS peaking coefficients,

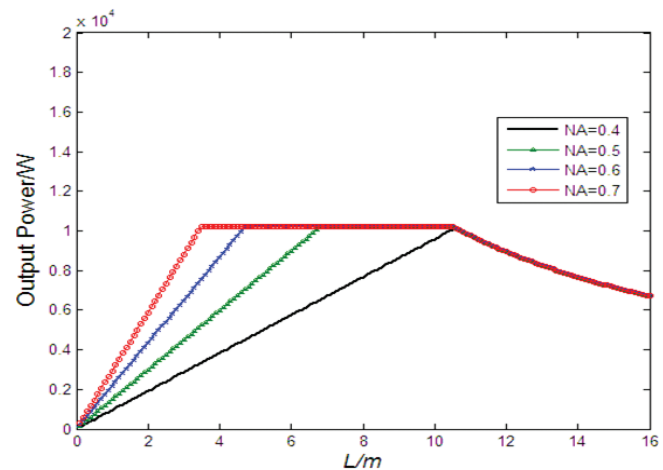


Fig. 3. Output power with different NA of inner cladding.

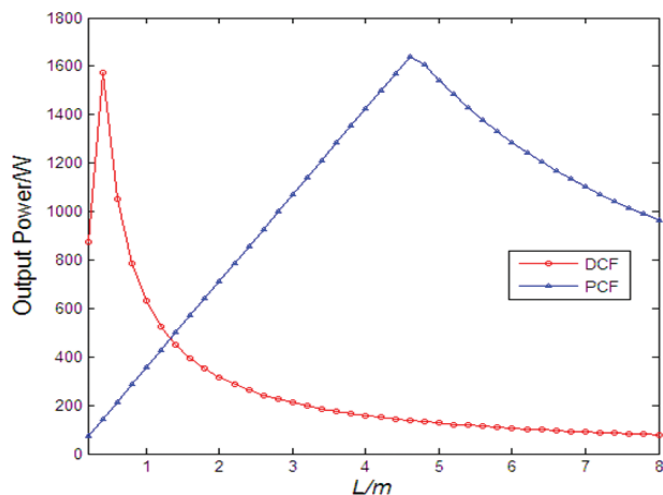


Fig. 4. Output powers of DCF and PCF working at single-mode and single-frequency conditions.

which means an improvement in the output power. This need to be further explored in future experiments.

In conclusion, ytterbium-doped PCFs have an endless single-mode characteristic and with the help of structural design, we can get nearly 100-kW power output in pure silica PCFs. The output power functioning in absolute single-frequency condition appears better than that of DCF and a 1.65-kW power output is expected. Increasing inner-cladding NA will help us to improve the output power, too.

This work was supported National University of Defense Technology under Grant No. JC12-07-03.

References

1. D. J. Richardson, J. Nilsson, and W. A. Clarkson, *J. Opt. Soc. Am. B* **27**, B63 (2010).
2. J. C. Knight, T. A. Birks, P. St. J. Russell, and D. M. Atkin, *Opt. Lett.* **21**, 1547 (1996).
3. P. Falkenstein, C. D. Merritt, and B. L. Justus, *Opt. Lett.* **29**, 1858 (2004).
4. T. A. Birks, J. C. Knight, and P. St. J. Russell, *Opt. Lett.* **22**, 961 (1997).
5. G. Imeshev and M. E. Fermann, *Opt. Express* **13**, 7424 (2005).
6. K. G. Hougaard, J. Broeng, and A. Bjarklev, *Electron. Lett.* **39**, 599 (2003).
7. R. F. Cregan, B. J. Mangan, J. C. Knight, T. A. Birks, P. S. Russell, P. J. Roberts, and D. C. Allan, *Science* **285**, 1537 (1999).
8. C. Wirth, O. Schmidt, A. Kliner, T. Schreiber, R. Eberhardt, and A. Tünnermann, *Opt. Lett.* **36**, 3061 (2011).
9. J. W. Dawson, M. J. Messerly, R. J. Beach, M. Y. Shverdin, E. A. Stappaerts, A. K. Sridharan, P. H. Pax, J. E. Heebner, C. W. Siders, and C. P. Barty, *Opt. Express* **16**, 13240 (2008).
10. D. Brown and H. J. Hoffman, *IEEE J. Set. Top Quantum Electron.* **2**, 207 (2001).
11. J. Limpert, T. Schreiber, A. Liem, S. Nolte, H. Zellmer, T. Peschel, V. Guyenot, and A. Tünnermann, *Opt. Express* **11**, 2982 (2003).
12. IPG Photonics, "PLD-100-A-9xx data sheet," <http://www.ipgphotonics.com> (2014).
13. TeraDiode, "TeraDiode-DLE-0970-00500-050-Datasheet," <http://www.teradiode.com> (2014).
14. NKT Photonics, "DC-135/14-PM-Yb," <http://www.NKTPhotonics.com> (2014).
15. C. Robin, I. Dajani, and B. Pulford, *Opt. Lett.* **39**, 666 (2014).